Biochemistry

 Volume 42, Number 31 August 12, 2003

Accelerated Publications

Sir2 Regulation by Nicotinamide Results from Switching between Base Exchange and Deacetylation Chemistry†

Anthony A. Sauve and Vern L. Schramm*

Department of Biochemistry, Albert Einstein College of Medicine, 1300 Morris Park Avenue, Bronx, New York 10461

Received June 4, 2003; Revised Manuscript Received June 19, 2003

ABSTRACT: Life span regulation and inhibition of gene silencing in yeast have been linked to nicotinamide effects on Sir2 enzymes. The Sir2 enzymes are NAD^+-dependent protein deacetylases that influence gene expression by forming deacetylated proteins, nicotinamide and 2′-*O*-acetyl-ADPR. Nicotinamide is a base-exchange substrate as well as a biologically effective inhibitor. Characterization of the base-exchange reaction reveals that nicotinamide regulates sirtuins by switching between deacetylation and base exchange. Nicotinamide switching is quantitated for the Sir2s from *Archeaglobus fulgidus* (Sir2Af2), *Saccharomyces cerevisiae* (Sir2p), and mouse (Sir2α). Inhibition of deacetylation was most effective for mouse Sir2α, suggesting species-dependent development of this regulatory mechanism. The Sir2s are proposed to form a relatively stable covalent intermediate between ADPR and the acetyl oxygen of the acetyllysine−protein substrate. During the lifetime of this intermediate, nicotinamide occupation of the catalytic site determines the fate of the covalent complex. Saturation of the nicotinamide site for mouse, yeast, and bacterial Sir2s causes 95, 65, and 21% of the intermediate, respectively, to return to acetylated protein. The fraction of the intermediate committed to deacetylation results from competition between the nicotinamide and the neighboring 2′-hydroxyl group at the opposite stereochemical face. Nicotinamide switching supports the previously proposed Sir2 catalytic mechanism and the existence of a 1′-*O*-peptidyl-ADPR·Sir2 intermediate. These findings suggest a strategy for increasing Sir2 enzyme catalytic activity *in vivo* by inhibition of chemical exchange but not deacetylation.

The Sir2 enzymes make up a newly classified family of NAD^+-dependent protein deacetylases that employ metabolically valuable NAD^+ as a substrate to convert acetyllysine side chains to unmodified lysine side chains in protein cosubstrates (*1*, *2*). The yeast Sir2 proteins were originally identified as coregulators of genetic silencing and are localized at chromatin in protein modules called Sir complexes. Within Sir complexes, these enzymes are believed to regulate chromatin structure (*3*, *4*) by the establishment and maintenance of hypoacetylation at H3 and H4 histone N-terminal tails (*5*−*7*). The role of these enzymes in regulating genetic information as part of a potent DNA-repressing machinery emphasizes their importance to the cell. Indeed, the Sir2 enzymes are broadly distributed across all phyla of life (*3*, *8*) and appear to have roles in the regulation of life span (*9*, *10*) and genomic stability (*8*). For example, Sir2 has been identified as being essential to life span extension caused by calorie restriction in *Saccharomyces cerevisiae* (*9*) and *Caenorhabditis elegans* (*10*) and impacts life span in *Drosophila* (*11*). Life span extension is caused by an increase in Sir2 activity during calorie

† Supported by NIH Grant AI34342.

* To whom correspondence should be addressed. E-mail: vern@aecom.yu.edu. Phone: (718) 430-2813. Fax: (718) 430-8565.

10.1021/bi034959l CCC: $25.00
Published on Web 07/17/2003

Scheme 1[a]

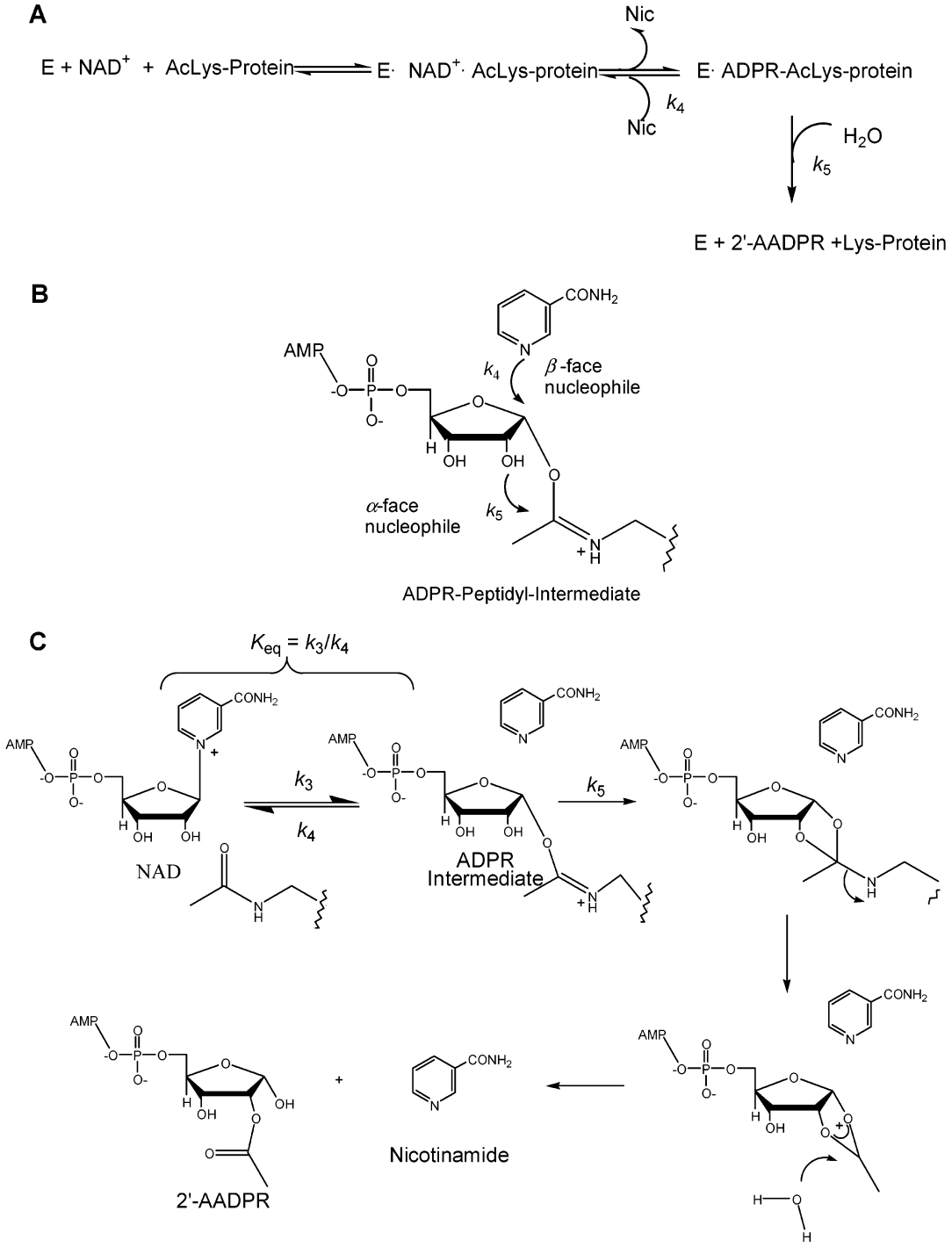

[a] Abbreviated reaction scheme for Sir2 deacetylation reactions. The competitive nucleophilic attacks on the Sir2 ADPR-peptidyl intermediate occur from both stereochemical faces (A and B). The top face of the ribosyl ring is designated β, and nicotinamide nucleophilic attack at C1′ leads to re-formation of β-NAD$^+$. The bottom face of the sugar is designated α, and the hydroxyl group attacks the α-amidate group from the same face to generate deacetylation products. The rate constants for the two competing nucleophilic attacks are shown as k_4 for exchange and k_5 for deacetylation (B). Reactions of Sir2 intermediates at saturating nicotinamide concentrations are shown with binding steps omitted (C).

restriction since additional copies of *SIR2* genes confer an increased longevity phenotype in *S. cerevisiae* (*9*) and *C. elegans* (*10*).

The mechanism by which Sir2 is activated by caloric restriction is not well understood, but an increased NAD$^+$/NADH ratio or an increased NAD$^+$ concentration has been suggested (*12*, *13*). A role for nicotinamide and the gene *PNC1* in regulating Sir2 activity has also been demonstrated (*6*, *14*, *15*). Pnc1 deamidates nicotinamide to form nicotinic acid and can lower levels of nicotinamide formed as a product of Sir2 and in pathways of NAD$^+$ metabolism (*6*, *14*, *15*). Pnc1 is overexpressed under several stress conditions (*15*−*17*) that increase longevity in yeast, implying that increased Pnc1 activity increases Sir2 action by reducing the level of nicotinamide inhibition. Nicotinamide is a potent inhibitor of Sir2 enzyme activity (*14*, *18*) and also serves as a base-exchange substrate of Sir2 enzymes (*18*−*20*). The relationship between nicotinamide base ex-

change, nicotinamide inhibition, and the reaction mechanism of Sir2 has not been defined, but is fundamental to regulation of Sir2 *in vivo*.

Sir2s have evolved a catalytically complex mechanism to involve NAD^+ and nicotinamide in an otherwise chemically simple *N*-deacetylase reaction. Reactions with peptide substrates produce the acetyl ester metabolites 2′- and 3′-*O*-acetyl-ADPR (*20*, *21*), nicotinamide, and deacetylated lysine side chains. The chemical mechanism that unites base-exchange and deacetylation reactions arises from a covalent 1′-*O*-α-peptidylamidate-ADPR intermediate that releases nicotinamide from the active site (*20*). This intermediate is sufficiently stable to permit regeneration of NAD^+ in the presence of elevated nicotinamide concentrations (Scheme 1A). This mechanism explains the requirement for the protein acetyllysine substrate to permit the base-exchange reaction and is consistent with all reliable information reported from active site mutagenesis studies, isotope labeling, and X-ray crystallography (*19*−*21*).

Here we characterize the base-exchange and inhibition kinetics for Sir2 enzymes from *Archeaglobus fulgidus* (Sir2Af2), *S. cerevisiae* (Sir2p), and mouse (Sir2α). These results establish that base exchange and nicotinamide inhibition are both consequences of the chemical reactivity of a single enzymatic intermediate. Interestingly, nicotinamide inhibition of yeast and bacterial enzyme deacetylation is incomplete at elevated nicotinamide concentrations. The inhibition patterns for all three enzymes can be explained by a reaction mechanism in which base exchange and deacetylation are competitive chemical processes emerging from the bifurcating reactivity of a Sir2 peptidyl-ADPR intermediate. This interpretation provides new insight into the chemical mechanism, reaction coordinate energetics, and regulation of the Sir2 enzymes. Strategies for increasing the catalytic deacetylation activity of Sir2 are apparent from this novel mechanism.

RESULTS

Kinetics of Nicotinamide Exchange and Inhibition. Several Sir2 enzymes have been shown to catalyze chemical exchange of radiolabeled nicotinamide into NAD^+ in the presence of an acetyllysine protein or peptide substrate (*18*−*20*). However, the kinetic and chemical mechanisms of base exchange have not been reported. Rates of Sir2-catalyzed exchange were measured as a function of [*carbonyl*-^{14}C]-nicotinamide concentration with saturating NAD^+ and peptide substrates (*20*). The K_m values for nicotinamide base exchange for the AF2, mouse, and yeast Sir2 enzymes were determined to be 36, 127, and 160 μM, respectively (Figure 1 and Table 1).

In the same experiments, ADPR and 3′-*O*-acetyl-ADPR products were measured to compare the rates of deacetylation reactions relative to base-exchange reactions in the mixtures. The production of these compounds is stoichiometrically linked with lysine deacetylation and can be used to quantify deacetylation (*20*−*23*). Deacetylation rates are expressed as a percentage of the uninhibited rate and plotted as a function of the nicotinamide concentration (Figure 2). Product formation rates decreased as nicotinamide concentrations were increased, but nicotinamide did not cause complete inhibition for the bacterial and yeast enzymes (Figure 2A). Approximately 79 and 35%, respectively, of the uninhibited rates remained at millimolar nicotinamide concentrations. For the mouse enzyme, >95% inhibition occurred at high nicotinamide concentrations (Figure 2A). Dixon plots ($1/v$ vs [I]) were hyperbolic for the AF2 and yeast enzymes, but linear for the mouse enzyme (Figure 2B,C). The K_m for NAD^+ for the three enzymes is in the range of 100−200 μM for these conditions. Increases in nicotinamide concentration to 2 mM did not alter the plateau for deacetylation or exchange rates for any of the three enzymes (data not shown, error of ±5%), demonstrating that nicotinamide competition for NAD^+ binding is in excess of 8 mM.

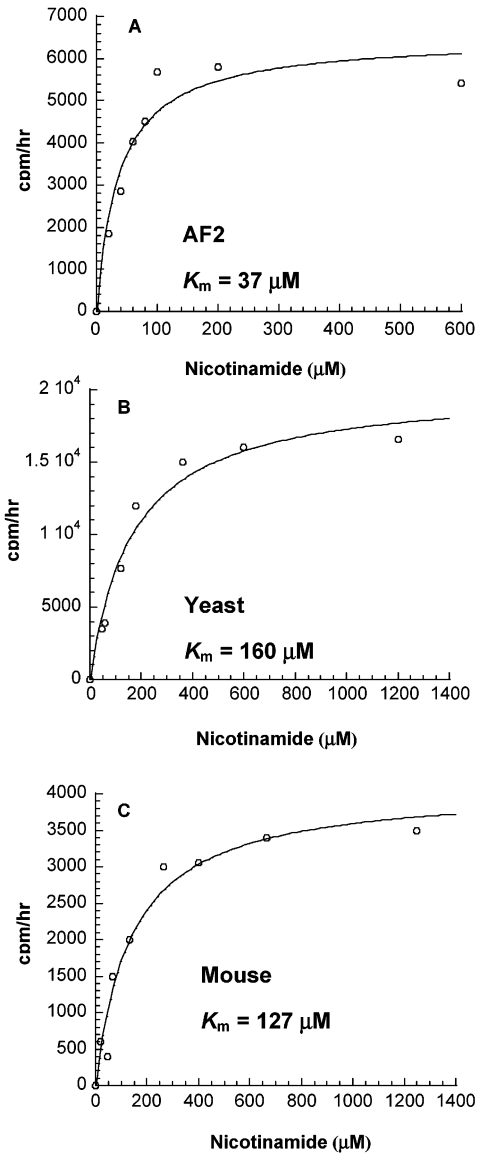

FIGURE 1: Exchange reaction rates vs nicotinamide concentration for the bacterial (A), yeast (B), and mouse (C) Sir2 enzymes. The lines are fits to the Michaelis−Menten equation.

Nicotinamide inhibition of bacterial and yeast enzymes was consistent with a noncompetitive interaction at a single binding site with a dissociation constant K_i. Fractional inhibition occurs by saturation of the site, expressed as $v = k_{cat} - k_p([I]/K_i + [I])$ for curves of v versus [I] and $1/v = 1/k_{cat} - k_p([I]/K_i + [I])$ for curves of $1/v$ versus [I], where v is the rate of deacetylation, [I] is the nicotinamide concentration, k_p is the extent to which the deacetylation reaction is decreased when the site is saturated, and k_{cat} is the deacety-

Table 1: Parameters for Inhibition, Exchange, and Deacetylation Reactions for Sir2 Enzymes[a]

enzyme	k_{cat}(deacetylation) (min^{-1})	k_{cat}(exchange) (min^{-1})	k_{inh}(deacetylation) (min^{-1})	K_m(exchange) (μM)	K_i(deacetylation) (μM)
bacterial	1.8 ± 0.2	0.35 ± 0.04	1.4 ± 0.2	37 ± 9	26 ± 4
yeast	1.8 ± 0.2	5.8 ± 0.4	0.60 ± 0.08	160 ± 36	120 ± 25
mouse	0.27 ± 0.03	3.0 ± 0.2	0.014 ± 0.002	127 ± 33	160 ± 50

[a] Reactions are initial rate measurements under conditions that saturate the enzyme [600 μM NAD and 300 μM peptide substrate (pH 7.8)]. The respective parameters are measured in the following ways. k_{cat}(deacetylation) is the rate of the deacetylation reaction for the enzyme in the absence of added nicotinamide. k_{cat}(exchange) is determined from the saturation curves for exchange shown in Figure 1. k_{inh}(deacetylation) is the residual deacetylation rate in the presence of 2 mM nicotinamide. The K_m(exchange) values are determined from the fits of the Michaelis−Menten equation to the plots in Figure 1. The K_i(deacetylation) values are derived from curve fits shown in Figures 2 and 3.

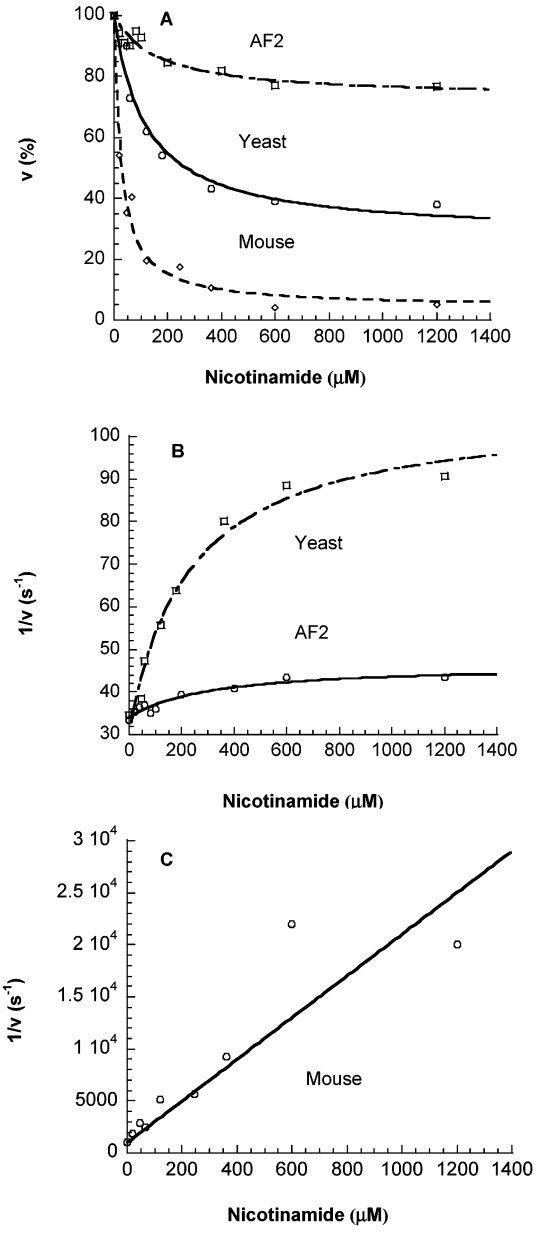

FIGURE 2: Deacetylation rate as a function of nicotinamide concentration. The lines were fit to the equation $v = k_{cat} - k_p([I]/K_i + [I])$ as defined in the text. The residual rate of deacetylation is the plateau (A). Dixon plots ($1/v$ vs [I]) of the deacetylation rates for yeast and AF2 enzymes (B) and for the mouse enzyme (C). Experimental data were fit to either a linear equation (C) or as defined in the text.

lation reaction rate at saturating NAD^+ and peptide concentrations with no inhibitor present. When $[I] \gg K_i$, the curve of v versus [I] asymptotically approaches the value k_{inh} (which equals $k_{cat} - k_p$) (Figure 2). Values for k_{inh}, the

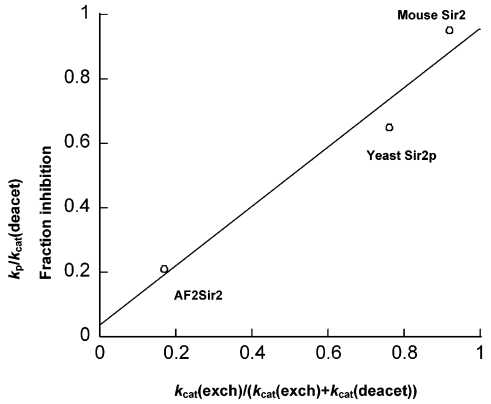

FIGURE 3: Correlation of fractional inhibition and fractional exchange for the three enzymes at nicotinamide site saturation.

residual deacetylation rate at nicotinamide saturation, are given in Table 1. Determinations of K_i allow comparison with K_m(exchange) for each enzyme. These values agree within experimental error, indicating that one site governs inhibition of deacetylation and base exchange (Table 1).

Species Specificity for Exchange and/or Acetyl Transfer. Comparisons of k_{cat}(exchange) and the corresponding k_{cat}(deacetylation) for each enzyme (Table 1) reveal that these parameters are enzyme specific. For the bacterial enzyme, the measured value of k_{cat}(exchange) is 5.1 times slower than k_{cat}(deacetylation). In contrast, for the yeast and mouse enzymes, the values of k_{cat}(exchange) exceed the values of k_{cat}(deacetylation) by 3.5- and 11-fold, respectively. The efficiency of exchange versus deacetylation is a predictor of inhibition; thus, the bacterial enzyme is modestly inhibited by nicotinamide, and the mouse enzyme is most inhibited (Figure 2A−C). This relationship is summarized in a plot of the ratio k_p/k_{cat}(deacetylation) versus k_{cat}(exchange)/[k_{cat}(deacetylation) + k_{cat}(exchange)] for the three enzymes (Figure 3). The near-linear relationship supports the proposal that exchange and deacetylation compete for a common intermediate according to rate constants k_4 and k_5, respectively (Scheme 1). The rate of deacetylation is maximal without nicotinamide, and its presence causes chemical reversal of the intermediate to the Michaelis complex.

Inhibiting the Base-Exchange Reaction. The nicotinamide switch between deacetylation and exchange predicts that nicotinamide analogues inert as exchange substrates will not significantly inhibit deacetylation since they cannot chemically trap the ADPR-peptidyl intermediate (Scheme 1). The nicotinamide analogues of Table 2 did not inhibit Sir2 deacetylation for bacterial or yeast enzymes at 5 mM, and only modest inhibition of the mouse enzyme was observed.

Table 2: Inhibition Properties of Nicotinamide Analogues in Sir2 Reactions

	Inhibition of exchange rate (%)[a]	Inhibition of deacetylation (%)[b]		
compound	yeast	bacterial	Yeast	mouse
Thionicotinamide 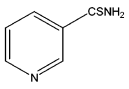	ND	4	15	16
Pyrazinamide 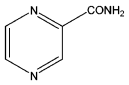	ND	4	1	1
Benzamide 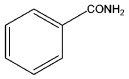	ND	5	0	44
Isonicotinamide 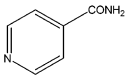	ND	4	0	18
Isonicotinamide[c]	40 ± 5[c] (n =6)		5 ± 5[c] (n =6)	

[a] Inhibition of the rate of nicotinamide base exchange at 320 μM [*carbonyl*-^{14}C]nicotinamide and 5 mM compound. [b] Inhibition of deacetylation in the presence of the given compound at 5 mM and no added nicotinamide. The errors of repeated measurements do not exceed ±10%. ND means no inhibition of exchange detected. [c] Conditions: 0.5 μM yeast Sir2, 42 mM isonicotinamide, 35 μM [*carbonyl*-^{14}C]nicotinamide, 1 mM NAD$^+$, and 300 μM peptide (pH 7.6). None of the compounds were base-exchange substrates.

None of the compounds that were tested were effective inhibitors of Sir2 base exchange for the yeast enzyme at a saturating nicotinamide concentration (Table 2). Special conditions where yeast Sir2 deacetylation and base exchange were performed in the presence of 35 μM [*carbonyl*-^{14}C]-nicotinamide and 42 mM isonicotinamide gave a 40% reduction in the exchange rate with a corresponding 5% decline in the deacetylation rate (Table 2).

Rate Constants for Intermediate Formation and Decomposition. The rate constants k_3-k_5 as defined in Scheme 1 for the mouse and yeast enzymes can be obtained with modest assumptions. For these enzymes, k_{cat}(exchange) > k_{cat}(deacetylation) by a factor of at least 3. Since they share a common rate constant k_3, $k_3 > k_5$ and $k_4 > k_5$ by a factor of at least 3. Therefore, we assume $k_5 = k_{cat}$(deacetylation). The relation $k_4/k_5 = k_{cat}$(exchange)/k_{int}, where k_{int} is the residual deacetylation rate, reflects the ratio of the two competing rates that deplete the ADPR intermediate. These ratios are 220, 9.8, and 0.25 for inhibition for the mouse, yeast, and bacterial enzymes, respectively. Calculation of k_4 using k_5 determines that k_3 is rate-limiting for exchange for the mouse and yeast enzymes. Therefore, the final rate can be approximated with the relation $k_3 = k_{inh} + k_{cat}$(exchange). These simple assumptions allow quantitation of k_{cat}(exchange), k_{cat}(deacetylation), and the residual rate k_{inh} (Table 3). The mechanistic assumptions can also derive the relation K_m(exchange) = K_i. This equality is analogous to that calculated and demonstrated for the ADPribosyl cyclase CD38 (*24*). The calculated rates assuming saturating conditions and equilibrium binding for peptide and NAD$^+$ agree to within 20% with the experimental values.

Table 3: Kinetic and Thermodynamic Parameters for Sir2 Reactions[a]

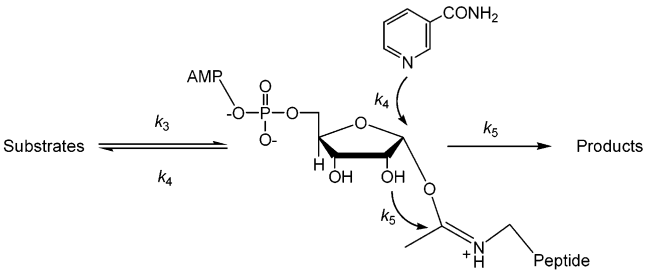

enzyme	k_4/k_5	k_3 (min^{-1})	k_4 (min^{-1})	k_5 (min^{-1})	K_{eq} (k_3/k_4)
bacterial	0.25	>1.8	0.25k_5	>1.8	ND
yeast	9.6	7.8	16.2	1.7	0.48
mouse	220	3.0	59.4	0.27	0.055

[a] The depicted rate constants and equilibrium parameters are defined according to the reaction. The parameters are calculated as follows. The k_4/k_5 ratio is calculated by the k_{cat}(exchange)/k_{inh}(deacetylation) ratio as defined in Table 1 and as explained in the text. For the yeast and mouse enzymes, the value of k_3 is determined by k_{cat}(exchange) + k_{inh}(deacetylation). The k_5 value is determined from k_{cat}(deacetylation). The value of k_4 is computed from the determined k_4/k_5 ratio and the value of k_5. The equilibrium constant is calculated from the rate constants k_3 and k_4. Assumptions are justified in the text and give errors for calculation of steady-state parameters of no more than 20%. Errors are determined from the individual steady-state parameters in Table 1. ND means the value cannot be determined.

DISCUSSION

Sir2 Biology. Sir2 enzymes use the central metabolite NAD$^+$ to deacetylate proteins that are modified and regulated by acetyllysine groups. Targets that have been identified for the Sir2 proteins include H3 and H4 histone N-terminal tails (*1*, *2*), p53 (*20*, *25*, *26*), tubulin (*27*), bacterial acyl-CoA synthetase (*28*), and the bacterial DNA binding protein Alba (*29*). Sir2 enzymes are proposed to be sensitive to global metabolic states of the cell with activity adjusted accordingly. In principle, because the enzyme utilizes NAD$^+$ as a substrate, it can be regulated by changes in intracellular NAD$^+$ levels (*12*, *13*). Alternatively, the NAD$^+$ metabolite nicotinamide can regulate Sir2 biochemical function *in vivo.* Recent biological studies in yeast support this view (*6*, *14*, *15*). Nicotinamide is a product of NAD$^+$ metabolism, a product in the Sir2 reaction, a base-exchange substrate (*18*−*20*), and an inhibitor of the Sir2 enzymatic reaction (*14*, *18*). According to the mechanism of Sir2 catalysis in Scheme 1, base-exchange catalysis must cause inhibition of Sir2 deacetylation because exchange depletes the enzyme of the ADPR intermediate that partitions between the exchange and deacetylation reactions.

Nature of the Covalent Intermediate. The ADPR intermediate is formed by an ADP ribosylation of the acyl oxygen of the acetyllysine substrate, and ^{18}O studies have established that a C1′−O bond is formed between the acyl oxygen and NAD$^+$ (*20*). Although this intermediate is chemically unusual and remains to be established by isolation or chemical trapping, the electrophilicity of an oxacarbenium ion transition state is sufficient to trap the weak nucleophile amide of the acetyl-peptide. Transition-state analysis of ADP ribosyl transfer reactions suggests that weak nucleophilic participation at the transition state is a general feature of these reactions and that the ADP ribosyl cation is indiscriminate

for nucleophiles (*30*, *31*). In addition, glycosyl amidates are reaction intermediates in glycosyltransferase reactions where they can form reversibly as reaction intermediates (*32*, *33*). The enzyme-bound intermediate has sufficient chemical reactivity to undergo reversal to re-form NAD^+ in the presence of nicotinamide. This exchange reaction is general to all Sir2 enzymes that have been examined (*18*, *19*). The intermediate also activates the amide to form the eventual deacetylation products: 2′-*O*-acetyl-ADPR and the deacetylated lysine substrate (*20*).

Single-Site Action of Nicotinamide. Saturation by nicotinamide does not compete for binding with NAD^+ or peptide at the concentrations that have been examined, consistent with a previous report (*14*). On the basis of the lack of nicotinamide inhibition of base-exchange reactions at 2 mM nicotinamide and the K_m values for NAD^+ with the three enzymes (100−200 μM), the K_i for competition between nicotinamide and NAD^+ is in excess of 8 mM. The inhibition of deacetylation by nicotinamide is entirely explained by the interaction of the base with the covalent intermediate to re-form NAD^+ and the acetyl protein. Although unusual, base reversal is precedented by the saturation kinetics for nicotinamide exchange for the ADP ribosyltransferase/cyclase enzyme CD38 (*24*).

Species-Dependent Inhibition by Nicotinamide. Yeast and bacterial Sir2s show partial inhibition by nicotinamide even at nicotinamide concentrations greater than $10K_i$ (data not shown). Deacetylation rates were reduced by 21 and 65%, respectively, but the mouse enzyme was inhibited 95% by nicotinamide with a K_i value of 160 μM. A single-site rapid-exchange binding model for nicotinamide that attenuates deacetylation and increases the level of exchange is consistent with all experimental data. The observation that mouse Sir2 is most inhibited suggests that the mammalian enzymes may be subjected to strong regulation by nicotinamide.

Mechanism of Partial versus Complete Nicotinamide Inhibition. Partial inhibition can occur in the covalent Sir2 mechanism if the intermediate reacts forward to products even if the nicotinamide site is saturated. In the related nicotinamide exchange and cyclization reactions catalyzed by CD38, complete inhibition of cyclization occurs at nicotinamide saturation because the covalent ADPR-Glu intermediate cannot cyclize until nicotinamide leaves the site (*24*, *34*). For CD38, the intermediate reacts only at the β-face and nicotinamide blocks access to other nucleophiles, while in the Sir2 intermediate, both α− and β-face reactions occur.

Chemical Partitioning of the Sir2 Intermediate. The dual reactivity of the Sir2-ADPR intermediate is demonstrated by the ability of the enzyme to catalyze both base-exchange and deacetylation chemistry from a common intermediate, even at saturating nicotinamide concentrations. The reactivity between exchange and deacetylation reactions occurs according to the rate constants k_4(exchange) and k_5(product formation) when nicotinamide is bound. This competition partitions the intermediate forward and backward to provide partial inhibition of deacetylation (Figure 2A,B). The independence of the deacetylation and exchange reactions establishes that exchange is a β-face nucleophile process, whereas deacetylation is an α-face nucleophilic process (Scheme 1B). ^{18}O studies have established that water does not attack the β-face at C1′, but acts as a nucleophile at the α-face, by attack of the acyl carbonyl carbon (Scheme 1C; *20*). In principle, these two stereofacially separated chemical processes can be sterically independent of each other, and can compete to deplete the intermediate on the enzyme.

Nicotinamide partition ratios are controlled by the relative rates of nucleophilic chemistry at the β-face versus the α-face of the intermediate. A plot of fractional inhibition versus the ratio of k_{cat}(exchange)/k_{cat}(deacetylation) shows that nicotinamide inhibition is strongly correlated to the ratio (Figure 3). The exchange and deacetylation reactions share the intermediate forming step k_3, and the ratio is determined by the chemical processes defined as k_4 for exchange and k_5 for deacetylation (Scheme 1C). Both k_4 and k_5 are slow; thus, rapid intermediate reactivity is unlikely to be the cause of incomplete inhibition by nicotinamide. The rate of exchange from the intermediate is faster than deacetylation steps in yeast and mouse enzymes and is slow relative to typical enzyme binding steps. Thus, separate bifacial competition for the reactive intermediate is the likely mechanism of nicotinamide inhibition. A prediction of this model is that nicotinamide analogues inhibit Sir2 enzymes according to their base-exchange behavior. Nicotinamide analogues are poor inhibitors of deacetylation, and are not base-exchange substrates (Table 2). An exception is the mouse enzyme, where an up to 45% reduction of the deacetylation rate is observed. For the yeast enzyme, these derivatives are also poor inhibitors of nicotinamide base exchange, suggesting poor binding to the intermediate or apo forms of the enzyme.

Changing the Deacetylation/Exchange Ratio. As proof of concept for manipulation of the exchange/deacetylation ratio, low nicotinamide and increased isonicotinamide concentrations led to a 40% reduction in the level of exchange versus control, but only a 5% reduction in the level of deacetylation (Table 2). Thus, base exchange can be inhibited preferentially over deacetylation. This result is consistent with the independence of chemical processes of the intermediate. Competitive binding of isonicotinamide and nicotinamide results in a decline in the extent of base exchange (β-face nucleophile chemistry) with little effect on deacetylation (α-face nucleophile chemistry).

Reaction Coordinate Diagrams for Sir2s. Reaction coordinate diagrams illustrate the energetic model of Sir2 catalysis and inhibition (Figure 4). The reaction coordinates for the mouse and yeast enzymes show that the ADPR intermediate is isolated by large energy barriers that account for the slow catalytic rates characteristic of the Sir2 enzymes. These barriers demonstrate the stable intermediate and the equilibration of binding steps of substrates and products. In the case of bacteria, the energy of the intermediate could not be established. Poor inhibition by nicotinamide may be barrier height modulation, an equilibrium effect in the first intermediate, or both. Increasing the energy of the intermediate increases the sensitivity of the enzyme intermediate to reversal by nicotinamide if the rate of deacetylation remains unchanged. The differences in the ability of nicotinamide to inhibit the mouse and yeast enzymes are due to the barriers between the ADPR intermediate, the Michaelis complex, and products. For the mouse enzyme, the equilibrium constant is in favor of the Michaelis complex and the level of inhibition by nicotinamide was >95% (Table 3). For the yeast enzyme, this equilibrium value is 0.48 and the level of inhibition by millimolar nicotinamide was 65% of the

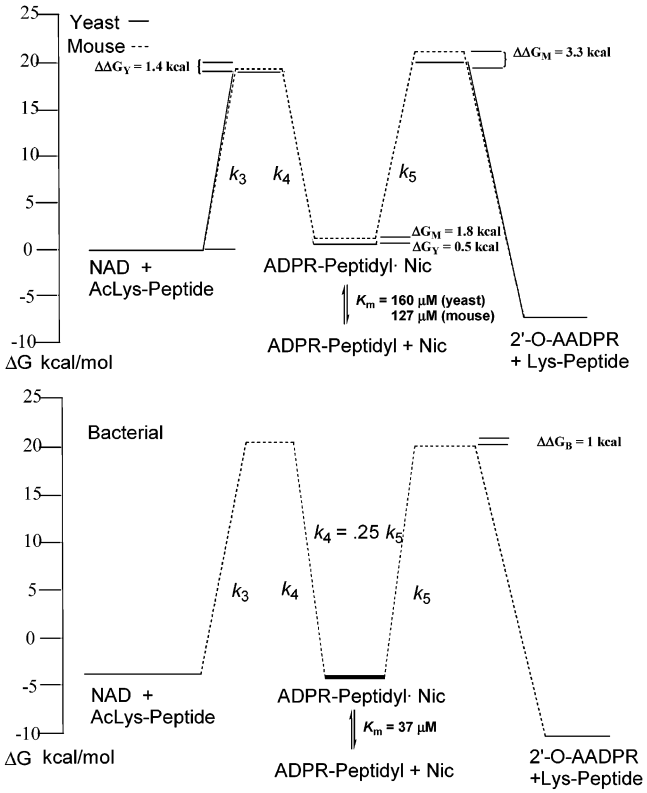

FIGURE 4: Reaction coordinates for Sir2 reactions based on values of k_3-k_5 of the bacterial, yeast, and mouse enzymes (Table 3). For the bacterial enzyme, only relative barrier heights are known and the relative energy of the intermediate is undetermined. Binding events are not shown. $\Delta G_M = \Delta G_M$(intermediate) $- \Delta G_M$(Michaelis). $\Delta G_Y = \Delta G_Y$(intermediate) $- \Delta G_Y$(Michaelis). $\Delta\Delta G_M = \Delta G_M$(hill 2) $- \Delta G_M$(hill 1). $\Delta\Delta G_Y = \Delta G_Y$(hill 2) $- \Delta G_Y$(hill 1). $\Delta\Delta G_B = \Delta G_B$(hill 1) $- \Delta G_B$(hill 2).

uninhibited rate. When nicotinamide concentrations are low, destabilization of the intermediate would not compromise catalytic efficiency, since the intermediate is trapped by dissociation of nicotinamide from the enzyme.

Conclusions. The mechanism of Sir2 catalysis presented here interprets the inhibition of nicotinamide to be a consequence of its chemical attack of a peptidyl-ADPR intermediate. The data can be analyzed completely with the proposed reaction mechanism for Sir2 base exchange and deacetylation (*20*). The findings suggest a chemical means for increasing the cellular activity of Sir2. Nicotinamide degradation has been suggested as a way to release Sir2 from inhibition (*6*). Alternatively, nicotinamide analogues capable of inhibiting base exchange but not deacetylation would cause *in vivo* activation of Sir2 and are currently under investigation.

MATERIALS AND METHODS

Yeast Sir2p was expressed from a plasmid generously provided by the Guarente laboratory (*2*). Bacterial Sir2Af2 was expressed from a plasmid generously provided by the Wolberger laboratory (*3*). The mouse Sir2α enzyme was obtained from Upstate Group in purified form. Reverse phase HPLC was performed on a Waters Delta 600 pump, a 717 autosampler, and a dual-wavelength 2486 detector. The p53 peptide was obtained from commercial sources.

SIR2-Exchange and Deacetylation Assays. Reaction mixtures of 50 μL of 50 mM potassium phosphate (pH 7.8) containing 300 μM KKGQSTSRHK(KAc)LMFKTEG peptide and 600 μM NAD^+ containing selected micromolar concentrations of [*carbonyl*-^{14}C]nicotinamide at 60 μCi/μmol (0, 10, 20, 30, 45, 60, 80, 90, 125, 250, 360, 600, and 1200) were reacted with 1 μM Sir2 enzyme added as a 1 μL addition of concentrated enzyme. After 2 h, 10 μL aliquots were removed at 0, 30, 60, 90, and 120 min. Each aliquot was combined with 50 μL of 50 mM ammonium acetate (pH 5.0) to quench and assayed by HPLC for deacetylation products and NAD^+. The chromatograms (260 nm) were obtained using 50 mM ammonium acetate (pH 5.0) as the eluant on a semipreparative Waters C-18 column (flow rate of 2.0 mL/min). Peaks for ADPR and 3′-*O*-acetyl-ADPR were quantified by integration. The peak for NAD^+ was collected and the radiation counted. Plots of rate versus nicotinamide concentration were fit using the curve $v = k_{cat}[S]/([S] + K_m)$ with the curve-fitting feature of Kaleidagraph. Plots of deacetylation rate versus nicotinamide concentration were fit to the equations described in the text. Experiments with 2 mM nicotinamide established the effects of this concentration on the deacetylation and exchange activity of the Sir2 enzyme.

Inhibition of Deacetylation with Nicotinamide Isosteres. Reactions were as described above, but mixtures for base reactions contained 5 mM pyrazinamide, isonicotinamide, thionicotinamide, or benzamide. Reactions were carried out (2 h for AF2 and yeast enzymes and 3 h for mouse enzyme) at 37 °C and quenched by addition of 80 μL of 50 mM ammonium acetate (pH 5.0). Product formation was quantified by HPLC. Thionicotinamide-NAD^+ was synthesized by CD38. Rates were compared with controls lacking added base.

ACKNOWLEDGMENT

We especially thank Dr. Jef Boeke for his interest and help in initiating this investigation.

REFERENCES

1. Landry, J., Sutton, A., Tafrov, S. T., Heller, R. C., Stebbins, J., Pillus, L., and Sternglanz, R. (2000) *Proc. Natl. Acad. Sci. U.S.A. 97*, 5807−5811.
2. Imai, S., Armstrong, C. M., Kaeberlain, M., and Guarente, L. (2000) *Nature 403*, 795−800.
3. Smith, J. S., Brachmann, C. B., Celic, I., Kenna, M. A., Muhammad, S., Starai, V. J., Avalos, J. L., Escalente-Semerena, J. C., Grubmeyer, C., Wolberger, C., and Boeke, J. D. (2000) *Proc. Natl. Acad. Sci. U.S.A. 97*, 6658−6663.
4. Rine, J., and Herskowitz, I. (1987) *Genetics 116*, 9−22.
5. Rusche, L. N., Kirchmaier, A. L., and Rine, J. (2003) *Annu. Rev. Biochem. 72*, 481−516.
6. Anderson, R. M., Bitterman, K. J., Wood, J. G., Medvedik, O., and Sinclair, D. A. (2003) *Nature 423*, 181−185.
7. Braunstein, M., Rose, A. B., Holmes, S. C., Allis, C. D., and Broach, J. R. (1993) *Genes Dev. 7*, 592−604.
8. Brachmann, C. B., Sherman, J. M., Devine, S. E., Comeron, E. E., Pillus, L., and Boeke, J. D. (1995) *Genes Dev. 9*, 2888−2902.
9. Lin, S. J., Deffossez, P. A., and Guarente, L. (2000) *Science 289*, 2126−2128.
10. Tissenbaum, H. A., and Guarente, L. (2000) *Nature 410*, 227−230.
11. Astrom, S. U., Cline, T. W., and Rine, J. (2003) *Genetics 163*, 931−937.
12. Lin, S. J., and Guarente, L. (2002) *Nature 418*, 344−348.
13. Campisi, J. (2000) *Science 289*, 2062−2063.

14. Bitterman, K. J., Anderson, R. M., Cohen, H. Y., Latorre-Esteves, M., and Sinclair, D. A. (2002) *J. Biol. Chem. 277*, 45099−45107.
15. Anderson, R. M., Bitterman, K. J., Wood, J. G., Medvedik, O., Cohen, H., Lin, S. S., Manchester, J. K., Gordon, J. I., and Sinclair, D. A. (2002) *J. Biol. Chem. 277*, 18881−18890.
16. Sinclair, D. A. (2002) *Mech. Ageing Dev. 123*, 857−867.
17. Gasch, A. P., Spellman, P. T., Kao, C. M., Carmel-Harel, O., Eisen, M. B., Storz, G., Botstein, D., and Brown, P. O. (2000) *Mol. Biol. Cell 11*, 4241−4257.
18. Landry, J., Slama, J. T., and Sternglanz, R. (2000) *Biochem. Biophys. Res. Commun. 278*, 685−690.
19. Min, J., Landry, J., Sternglanz, R., and Xu, R. M. (2001) *Cell 105*, 269−279.
20. Sauve, A. A., Celic, I., Avalos, J., Boeke, J. D., and Schramm, V. L. (2001) *Biochemistry 40*, 15456−15463.
21. Jackson, M. D., and Denu, J. M. (2002) *J. Biol. Chem. 277*, 18535−18544.
22. Tanner, K. G., Landry, J., Sternglanz, R., and Denu, J. M. (2000) *Proc. Natl. Acad. Sci. U.S.A. 97*, 14178−14182.
23. Tanny, J. C., and Moazed, D. (2001) *Proc. Natl. Acad. Sci. U.S.A. 98*, 415−420.
24. Sauve, A. A., Munshi, C., Lee, H. C., and Schramm, V. L. (1998) *Biochemistry 37*, 13239−13249.
25. Vaziri, H., Dessain, S. K., Eaton, E. N., Imai, S. I., Frye, R. A., Pandita, T. K., Guarente, L., and Weinberg, R. A. (2001) *Cell 107*, 149−159.
26. Luo, J., Nikolaev, A. Y., Imai, S., Chen, D., Su, F., Shiloh, A., Guarente, L., and Gu, W. (2001) *Cell 107*, 137−148.
27. North, B. J., Marshall, B. L., Borra, M. T., Denu, J. M., and Verdin, E. (2003) *Mol. Cell 2*, 437−444.
28. Starai, V. J., Celic, I., Cole, R. N., Boeke, J. D., and Escalante-Semerena, J. C. (2003) *Science 298*, 2390−2392.
29. Bell, S. D., Botting, C. H., Wardleworth, B. N., Jackson, S. P., and White, M. F. (2002) *Science 296*, 148−151.
30. Berti, P. J., and Schramm, V. L. (1997) *J. Am. Chem. Soc. 119*, 12069−12078.
31. Scheuring, J., and Schramm, V. L. (1997) *Biochemistry 36*, 4526−4534.
32. Knapp, S., Vocadlo, D., Gao, Z., Kirk, B., Lou, J., and Withers, S. G. (1996) *J. Am. Chem. Soc. 118*, 6804−6805.
33. Zechel, D. L., and Withers, S. G. (2000) *Acc. Chem. Res. 33*, 11−18.
34. Sauve, A. A., Deng, H., Angeletti, R. H., and Schramm, V. L. (2000) *J. Am. Chem. Soc. 122*, 7855−7859.

BI034959L